

This article was downloaded by: [University of California, San Diego]

On: 21 August 2012, At: 11:51

Publisher: Taylor & Francis

Informa Ltd Registered in England and Wales Registered Number: 1072954 Registered office: Mortimer House, 37-41 Mortimer Street, London W1T 3JH, UK



Molecular Crystals and Liquid Crystals Science and Technology. Section A. Molecular Crystals and Liquid Crystals

Publication details, including instructions for authors and subscription information:

<http://www.tandfonline.com/loi/gmcl19>

The Effect of Material Parameters on the Hysteresis of Bistable STN Displays

Jianlin Li^a, Charles D. Hoke^a & Philip J. Bos^a

^a Liquid Crystal Institute, Kent State University, Kent, Ohio, 44242, USA

Version of record first published: 04 Oct 2006

To cite this article: Jianlin Li, Charles D. Hoke & Philip J. Bos (1997): The Effect of Material Parameters on the Hysteresis of Bistable STN Displays, Molecular Crystals and Liquid Crystals Science and Technology. Section A. Molecular Crystals and Liquid Crystals, 304:1, 113-124

To link to this article: <http://dx.doi.org/10.1080/10587259708046951>

PLEASE SCROLL DOWN FOR ARTICLE

Full terms and conditions of use: <http://www.tandfonline.com/page/terms-and-conditions>

This article may be used for research, teaching, and private study purposes. Any substantial or systematic reproduction, redistribution, reselling, loan, sub-licensing, systematic supply, or distribution in any form to anyone is expressly forbidden.

The publisher does not give any warranty express or implied or make any representation that the contents will be complete or accurate or up to date. The accuracy of any instructions, formulae, and drug doses should be independently verified with primary sources. The publisher shall not be liable for any loss, actions, claims, proceedings, demand, or costs or damages whatsoever or howsoever caused arising directly or indirectly in connection with or arising out of the use of this material.

THE EFFECT OF MATERIAL PARAMETERS ON THE HYSTERESIS OF BISTABLE STN DISPLAYS

JIANLIN LI, CHARLES D. HOKE AND PHILIP J. BOS

Liquid Crystal Institute, Kent State University, Kent, Ohio 44242, USA

Abstract We have investigated the hysteretic electro-optic behavior of super-twisted nematic (STN) displays with the twist angles larger than 270° . A pair of Lagrange's equations based on the continuum theory were solved numerically. The Gibbs energy and elastic energy of the nematic liquid crystal medium under the influence of external electric field were calculated. The director configurations at an applied field may be significantly different depending on the initial conditions. The elastic energy of the liquid crystal medium is used to describe its bistability. The total Gibbs energy, which represents the stability of the system, is discussed with each bistable state. The effects of cell twist angle, elastic constants, thickness to pitch ratio, dielectric parameter, and surface pretilt angle are presented.

INTRODUCTION

The hysteresis of electro-optic curves of nematic liquid crystals with twist angles larger than 270° was discovered in early 1980s.^{1,2,3} When the twist angle is increased, the voltage applied to the cell required to deform the planar state increases due to the higher elastic distortion. At the same time, the voltage required to hold the system to 'homeotropic' state is independent of the twist angle. When the twist angle is larger than 270° , in which case the two voltages are almost the same, the deforming voltage for planar state becomes larger than the holding voltage for homeotropic state.⁴ In other words, the hysteresis appears in the region between these two voltages when the twist angle is larger than 270° . A study trying to better understand the physics of bistability would be very helpful for the design of a device, which utilizes the hysteresis of highly-twisted nematic and has the advantages of low-driving voltage, fast switching characteristics and disclination-free appearance.^{5,6,7} It would also be very useful for the

design of state-of-the-art STN displays (260° to 270° twist) for choosing the right device and material parameters to minimize the possible hysteresis, which would destroy the high multiplexity of a STN LCD. The mechanism for the bistability of this type of device is different from the textural changes of cholesteric liquid crystal displays.^{8,9} A qualitative explanation of the switching mechanism for a 360° twist cell was given by using the mid-plane tilt angle's 'up' and 'down' states.¹⁰ Our theoretical model, used for determining the complete director configuration and energy densities of a TN, STN, or Cholesteric display, is based on the continuum theory. The Lagrange's equations are solved by using a numerical relaxation technique. With the results from this technique, we discuss the elastic energy and the total Gibbs energy of the system and their respective implication of bistability and stability. Depending on the initial conditions, the elastic energies for the same applied voltage in the hysteresis region could be completely different due to the different director configurations. The effects of different display and material parameters on the bistability and driving voltages are calculated and discussed.

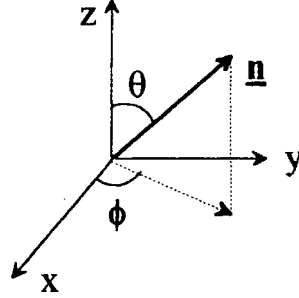
THEORETICAL MODEL

From the continuum theory, the free energy density in a liquid crystal medium (neglecting the surface divergence terms for K_{13} and K_{24}) has the form:

$$F = \frac{1}{2} \{ K_1 (\nabla \cdot \mathbf{n})^2 + K_2 [\mathbf{n} \cdot (\nabla \times \mathbf{n}) - q_0]^2 + K_3 [\mathbf{n} \times (\nabla \times \mathbf{n})]^2 \} - \frac{1}{2} (\mathbf{D} \cdot \mathbf{E}) - \frac{1}{2} (\mathbf{B} \cdot \mathbf{H}) \quad (1)$$

where K_1 , K_2 and K_3 are splay, twist and bend elastic constants, respectively; \mathbf{n} is the director; \mathbf{D} , \mathbf{E} , \mathbf{B} and \mathbf{H} are the electric displacement, the electric field, the magnetic induction and the magnetic field, respectively; q_0 is the wave vector which is equal to $2\pi/P$ and P is the nature pitch. The positive and negative values of q_0 correspond to the left and right handed helix, respectively.

For a system with the director $\mathbf{n} = (\sin\theta\cos\phi, \sin\theta\sin\phi, \cos\theta)$, where θ is the polar angle and ϕ is the azimuthal angle (see Figure 1), if the liquid crystal layer is enclosed between two parallel glass plates, θ and ϕ would only be a function of z .

FIGURE 1 Coordinates for liquid crystal director \underline{n}

The free energy density can be written as,

$$F = \frac{1}{2} \{ K_1 (\sin^2 \theta) \bullet (\theta')^2 + K_2 [(\sin^4 \theta) \bullet (\phi')^2 + 2q_0 (\sin^2 \theta) \bullet (\phi') + q_0^2] + K_3 [(\cos^2 \theta) \bullet (\theta')^2 + (\sin^2 \theta \cos^2 \theta) \bullet (\phi')^2] \} - \frac{1}{2} (\underline{D} \bullet \underline{E}) - \frac{1}{2} (\underline{B} \bullet \underline{H}) \quad (1')$$

Assuming the electric field is applied along the z axis and the magnetic field is absent, the z component of \underline{D} is a constant as

$$D_z = \underline{D} \bullet \hat{k} = \epsilon_0 \{ \epsilon_{//} (\underline{E} \bullet \underline{n}) \underline{n} + \epsilon_{\perp} [\underline{E} - (\underline{E} \bullet \underline{n}) \underline{n}] \} \bullet \hat{k} = \epsilon_0 (\epsilon_{//} \cos^2 \theta + \epsilon_{\perp} \sin^2 \theta) E,$$

i.e. Equation (1') yields

$$F = \frac{1}{2} \{ K_1 (\sin^2 \theta) \bullet (\theta')^2 + K_2 [(\sin^4 \theta) \bullet (\phi')^2 + 2q_0 (\sin^2 \theta) \bullet (\phi') + q_0^2] + K_3 [(\cos^2 \theta) \bullet (\theta')^2 + (\sin^2 \theta \cos^2 \theta) \bullet (\phi')^2] \} - \frac{D_z^2}{2\epsilon_0 (\epsilon_{//} \cos^2 \theta + \epsilon_{\perp} \sin^2 \theta)} \quad (2)$$

In order to obtain how the director is configured under the influence of an electric field, one needs to minimize the energy density using Lagrange's equations for θ and ϕ , which are the bulk torque balances between elastic energy and external field energy at equilibrium

$$\frac{\delta F}{\delta \theta} = \frac{\partial F}{\partial \theta} - \frac{d}{dz} \frac{\partial F}{\partial \theta'} = 0$$

$$\frac{\delta F}{\delta \phi} = \frac{\partial F}{\partial \phi} - \frac{d}{dz} \frac{\partial F}{\partial \phi'} = 0$$

It would be very difficult to obtain any analytical results for these two equations without making some kinds of assumptions about the mid-plane director and the general shape of the director configuration. We solve this problem by treating a pair of dynamic equations of liquid crystal¹¹

$$\frac{\delta F}{\delta \theta} = -v \frac{\partial \theta}{\partial t} \quad (3)$$

$$\frac{\delta F}{\delta \phi} = -v \sin^2 \theta \frac{\partial \phi}{\partial t} \quad (4)$$

where v is the viscosity coefficient, to find the director configuration numerically.

Substituting terms obtained from Equation (2), Equations (3) and (4) can be written as

$$\begin{aligned} v \frac{\partial \theta}{\partial t} = & [K_1(\sin^2 \theta) + K_3(\cos^2 \theta)] \bullet (\theta'') + [K_1 - K_3](\sin \theta \cos \theta) \bullet (\theta')^2 \\ & - \{ [2K_2 \sin^2 \theta + K_3(\cos 2\theta)] \bullet (\phi')^2 - 2K_2 q_0(\phi') \\ & + \frac{D_z^2}{\epsilon_0} \left[\frac{\Delta \epsilon}{(\epsilon_{//} \cos^2 \theta + \epsilon_{\perp} \sin^2 \theta)^2} \right] \} (\sin \theta \cos \theta) \end{aligned} \quad (5)$$

and

$$\begin{aligned} v \sin^2 \theta \frac{\partial \phi}{\partial t} = & [K_2(\sin^4 \theta) + K_3(\sin^2 \theta \cos^2 \theta)] \bullet (\phi'') + 2[K_2 q_0 \sin \theta \cos \theta] \bullet (\theta') \\ & + 2[2K_2 \sin^2 \theta + K_3(\cos 2\theta)](\sin \theta \cos \theta) \bullet (\theta' \phi') \end{aligned} \quad (6)$$

The coupled Equations (5) and (6) are solved numerically by letting $\theta(z)$ and $\phi(z)$ relax to equilibrium.

RESULTS AND DISCUSSIONS

The hysteresis behavior of the system was simulated by sweeping the applied voltage from 0 V to 5 V and then back to 0 V. The material constants for liquid crystal ZLI-1694 were used for the studies. The surface condition was assumed as hard anchoring, as commonly used in display modeling programs. The twist angle and the pretilt angle of the cell were 360° and 5° , respectively. The thickness to pitch ratio was 0.88. In this process, the director configurations, the system free energy and the elastic energy were obtained as a function of applied voltage with the increment of 0.1 V.

In Figure 2(a) and 2(b), where the obtained director configurations are plotted, two different director configurations exist for the same voltage in the region between 2.1 V to 2.9 V. When the applied voltage is increased from 0 V to less than 2.9 V, the director configurations are almost identical with the mid-cell tilt angle parallel to the surface; when the applied voltage reaches 3.0 V, the effect of applied electric field causes the director configuration to have a significant different shape than that of 2.9 V, with the mid-cell tilt angle almost perpendicular to the substrate surface. On the other hand, when the applied field is decreased from 5.0 V, the mid-plane tilt angle stays perpendicular to the surface until the applied voltage drops down to 2.0 V. During the process, the magnitude of the polar angle gradient has the largest value at the surface and becomes smaller gradually to mid-cell. At 2.1 V, the gradient throughout the cell has the same magnitude except at the mid-cell, where it is still zero. The optical effect of the different director configurations is that the display could be bright or dark in between a pair of crossed polarizers depending on initial voltages.

In Figure 3(a), a plot of elastic energy and Gibbs free energy, defined as the elastic energy density minus the electrostatic energy density in the liquid crystal, is shown as a function of applied voltage. The hysteretic characteristics are also seen in both of these energy curves from 2.1 V to 2.9 V, with the elastic energy demonstrating a much more profound effect and making it a better quantity to describe the hysteresis of a highly twisted nematic. The total Gibbs free energy, which represents the stability of the system, has a cross at the high-voltage end of the hysteresis loop. This means that the system considered favors the mid-cell director parallel to the surface, if a holding voltage

is applied to realize the bistability. This was observed experimentally.⁷ One can obtain a crossover voltage inside the hysteresis loop by varying the device and/or material parameters as illustrated in Figure 3 (b). If the holding voltage is tuned to this crossover voltage, the system would be in such a balance that it does not favor either bistable state.

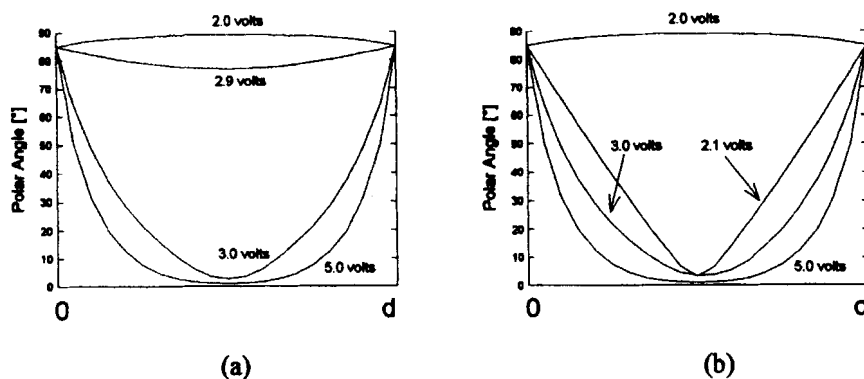


FIGURE 2 Director configurations (polar angle) showing the hysteresis of a 360° twist nematic cell (liquid crystal material ZLI-1694). (a) Applied voltage increases from 0 V to 5 V; (b) Applied voltage decreases from 5 V to 0 V.

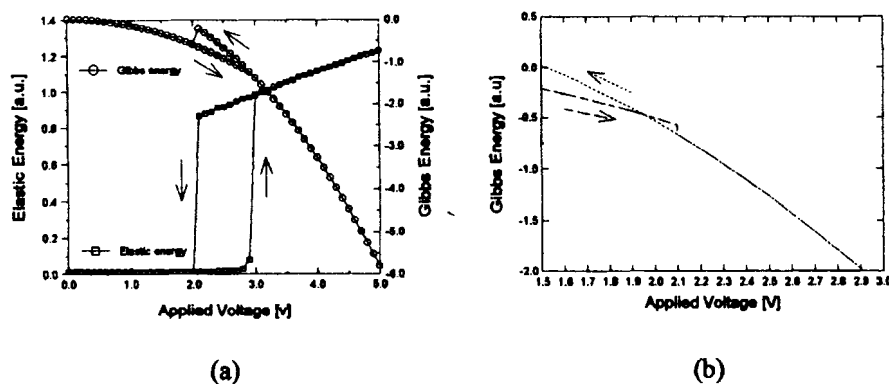


FIGURE 3 (a) Elastic and total Gibbs energies of the cell with 5° pretilt; (b) Total Gibbs energy of a cell with 35° pretilt, as a function of applied voltage.

In Figure 4(a), the azimuthal angle distribution of the director configuration at 2.1 V with high field initial condition is shown along with the polar angle distribution. The rate of the twist decreases from the surfaces to about one-quarter into the cell and then increases with the most of the change occurs at mid-cell. How far into the cell from the surface this rate decreases depends on the percentage of chiral additive and the bend/splay elastic constant ratio.

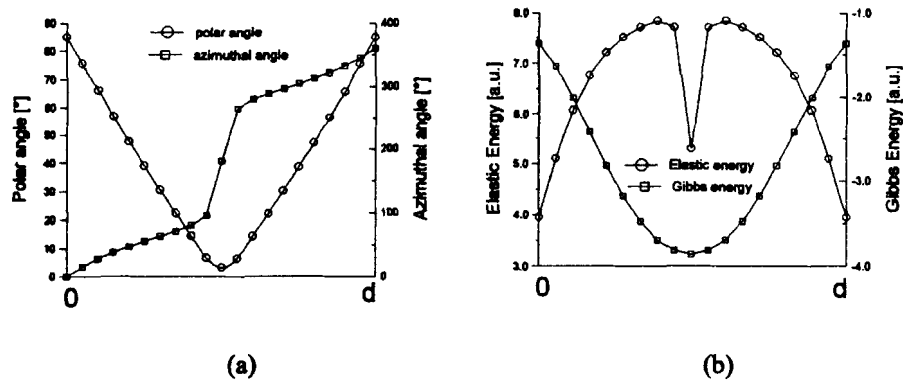


FIGURE 4 (a) Director configuration and (b) elastic and Gibbs energies at 2.1 V applied voltage, with the high-field initial condition.

A further investigation of elastic energy distribution inside a cell explains that the center director prefers to be perpendicular to the surface with the high-field initial condition. When the applied voltage is high, e.g. 5 V, the elastic energy density distribution is parabolic with the lowest energy density at the center. The general shape of the elastic energy distribution stays about the same when the applied voltage is decreased from 5 V, while a energy well at the center forms. A plot demonstrating the energy well is shown in Fig. 4(b), where the Gibbs energy is also plotted. This energy well at the center of the cell shows that the director at mid-cell prefers to be perpendicular to the surfaces and is stable. There is a flat elastic energy distribution at the same applied voltage of 2.1 V with the zero field initial condition. We believe that methods of inducing the mid-plane director to align perpendicular to the surface will increase the width of hysteresis curves.

The stability of this energy well with respect to the asymmetrical condition is studied with a cell of different surface pretilts (5° at one surface and 10° at another surface). The hysteresis is compared with the result of cells with the same pretilt angles (5° for one and 10° for another) on both surfaces, shown in Figure 5. Except for the minor shift of drive voltages and very slight increase of the hysteresis, there is no significant difference between the three curves. The minor change is due to the differences in pretilt angle magnitudes. This is also evident in the Gibbs energy curves.

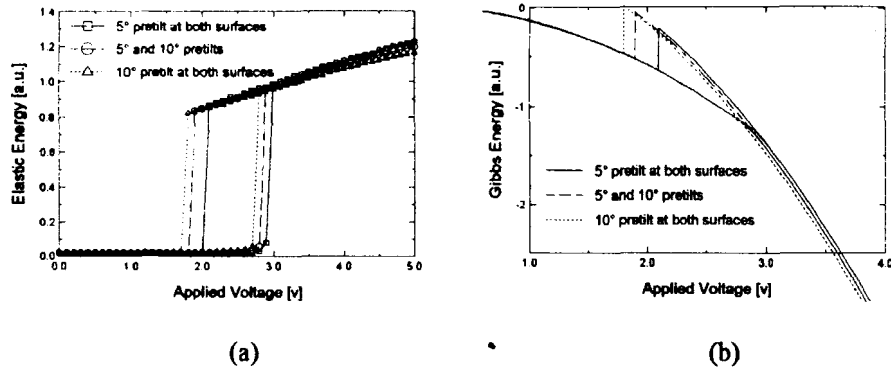


FIGURE 5 Comparison of hysteresis for 360° twist devices with same and different pretilt angles at two surfaces: (a) elastic energies and (b) Gibbs energies.

Besides the device parameter twist angle, changing other material parameters such as surface pretilt angle, bend/splay elastic constant ratio (k_3/k_1), twist/splay elastic constant ratio (k_2/k_1) and dielectric parameter as well as the device/material parameter thickness to pitch ratio (d/p), will have an effect on the electro-optic curves. We will summarize the results from our study, which systematically varies these parameters from the standard reference values. The standard reference condition for making comparisons is a cell with twist angle of 360° , surface pretilt of 5° , d/p ratio of 0.88, contains liquid crystal material ZLI-1694 from E. Merck, with material constants of $k_3/k_1=1.31$, $k_2/k_1=0.47$ and $\gamma=1.67$.

When the twist angles are larger than 270° , infinite steepness is the common property for electro-optic curves.⁴ Figure 6(a) illustrates the effect of twist angle on the hysteresis and drive voltage, which is defined as the minimum voltage that induces noticeable change in the director configuration with zero field initial condition. Increasing the twist angle causes the increase of drive voltage and hysteresis. It also pushes the crossover point inward inside the hysteresis loop, as shown in Figure 7(a).

Pretilt angle: With the increase of the surface pretilt, the drive voltage decreases as the normal STN and hysteresis increases. The hysteresis curves for pretilt angles of 5° , 10° and 20° are shown in Figure 6(b). Increasing the pretilt also decreases the stability of the system if a holding voltage is applied at the middle of the hysteresis loop, as shown in Figure 7(b).

Thickness to pitch ratio d/p : The lower d/p ratio produces lower drive voltage and wider hysteresis curve. The curves for d/p of 0.75, 0.88 and 1.00 (360° twist) are plotted in the Figure 6(c). Lowering this ratio will push the crossover point inward very slightly, as shown in Figure 7(a).

As shown in Figure 6(d), increasing the bend/splay elastic constant ratio k_3/k_1 (while keeping k_2/k_1 constant) will not only increases the drive voltage, but also decreases the fall-off voltage, hence increasing the hysteresis of the device. Increasing this ratio will decrease the stability of the bistable state if a holding voltage of the same value is applied since the energy differences between the two states increases as shown in Figure 7(d).

The twist/splay elastic constant ratio k_2/k_1 (while keeping k_3/k_1 constant) effect on bistability was studied for a range between 0.4 to 0.6. Curves of elastic energy as a function of applied voltage are plotted on Figure 6(e). Decreasing this ratio increases the hysteresis by decreasing the fall-off voltage, but does not change the drive voltage. It also moves the crossover voltage inward, as shown in Figure 7(e).

The effect of dielectric parameter on bistability is that decreasing γ increases the hysteresis and decreases the drive voltage of the device as shown in the Figure 6(f). Decreasing γ also decreases the crossover voltage from the high-voltage end of the hysteresis loop, as shown in Figure 7(f).

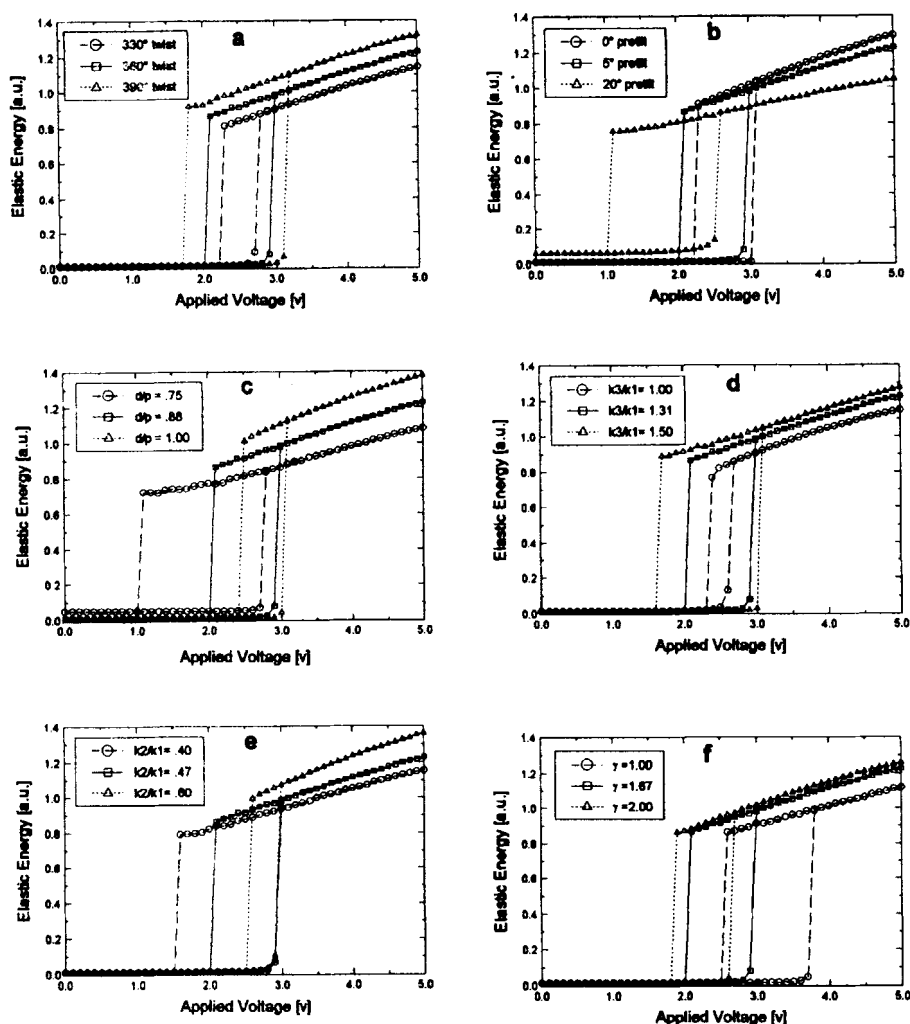


FIGURE 6 Effect of device and material parameters on the shape of the electro-optic curve. In each set of curves, one parameter is varied: (a) twist angle; (b) pretilt angle; (c) thickness to pitch ratio; (d) bend/splay elastic constant ratio; (e) twist/splay elastic constant ratio; (f) dielectric parameter γ . The standard condition curve, common to all figures, refers to the parameter set twist=360°, pretilt=5°, d/p=0.88, $k_3/k_1=1.31$, $k_2/k_1=0.47$ and $\gamma=1.67$.

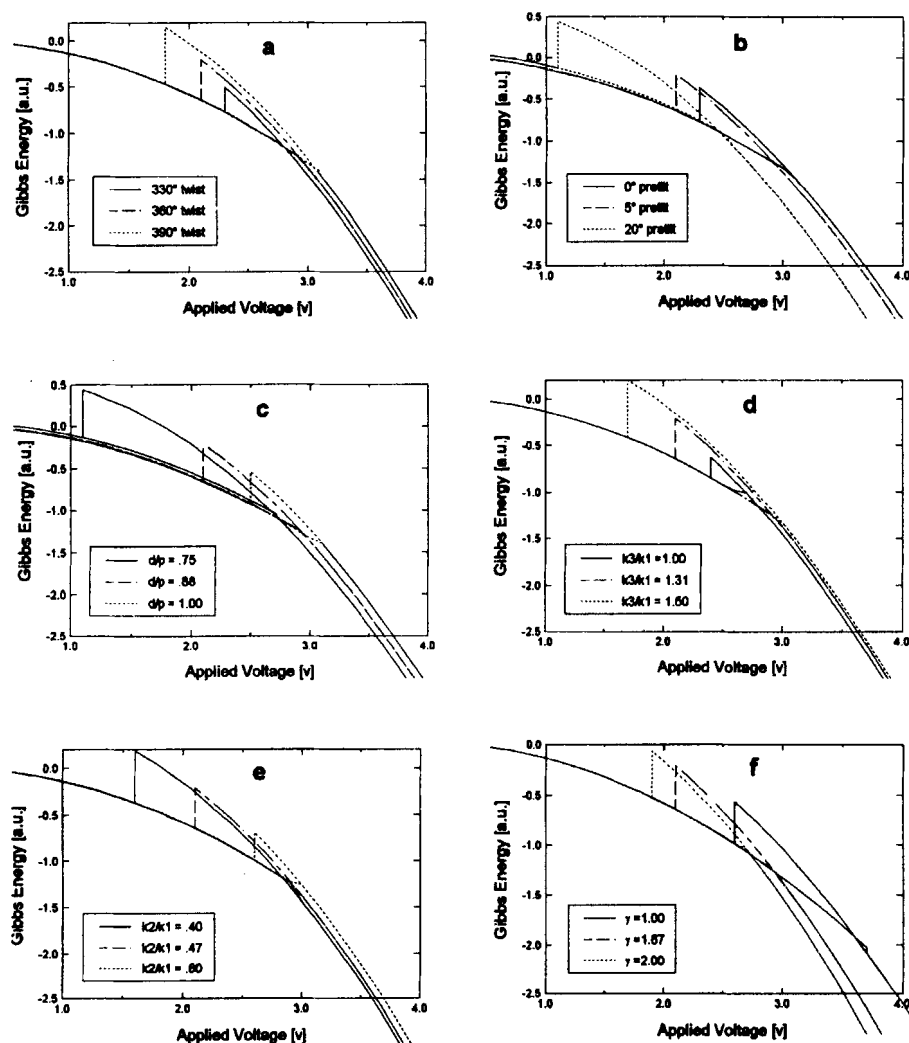


FIGURE 7 Effect of device and material parameters on the stability of the bistable states. The conditions are the same as in Figure 6.

CONCLUSIONS

A numerical relaxation technique that minimizes the liquid crystal system free energy was presented in detail. The elastic energy is found to be most suitable for describing the bistability of highly twisted nematics. The stability of mid-cell director having a direction perpendicular to the surface is found to control the hysteresis loop width. The device and material parameters, such as surface pretilt angle, bend/splay elastic constant ratio (k_3/k_1), twist/splay elastic constant ratio (k_2/k_1) and the dielectric parameter as well as the thickness-to-pitch ratio (d/p), exhibit impacts on the drive voltage, hysteresis width and stability of bistable states. Based upon the results of this study, various techniques that might stabilize the mid-cell director are being studied.

ACKNOWLEDGMENTS

Research supported by NSF ALCOM Center under the grant # 89-20147.

REFERENCES

1. D. W. Berreman and W. R. Heffner, *J. Appl. Phys.*, **52**, 3032(1981).
2. D. W. Berreman and W. R. Heffner, *Appl. Phys. Lett.*, **37**, 109(1980).
3. P. A. Breddels and H. A. van Sprang, *J. Appl. Phys.*, **58**, 2162(1985).
4. T. Scheffer and J. Nehring, in *Liquid Crystals: Applications and Uses*, ed. B. Bahadur, (World Scientific, London, 1990), Vol. 1, p.251.
5. H. A. van Sprang, R. G. Aartsen, and A. J. S. M. de Vaan, *J. Appl. Phys.*, **59**, 3087(1986).
6. T. Tanaka, Y. Sato, A. Inoue, Y. Momose, H. Nomura, S. Lino, *Asia Display '95*, 259(1995).
7. J. Li, C.D. Hoke, D.S. Fredley, and P.J. Bos, *SID '96*, 265(1996).
8. W. R. Heffner and D. W. Berreman, *J. Appl. Phys.*, **53**, 8599(1982).
9. P.G. de Gennes and J. Prost, *The Physics of Liquid Crystals*, 2nd Ed., 1993.
10. D. W. Berreman and W. R. Heffner, *Proceedings of the SID*, **22**, 191(1981).
11. J. Li, *Ph.D. Dissertation*, Kent State University, 113(1994).